Article

Synthesis and Characterization of [PtIn](GeO)O and Its Solid Solution [PtIn](GaO)(GeO)O (0 ≤ *x* ≤ 2): Gradual Color Change of the Solid Solution from Black (*x* = 0) to Yellow (*x* = 2) as a Consequence of Quantum Dot Effect

Jrgen Khler, Holger Friedrich, Myung-Hwan Whangbo, and Antoine Villesuzanne

J. Am. Chem. Soc., **2005**, 127 (37), 12990-12996• DOI: 10.1021/ja053280x • Publication Date (Web): 24 August 2005

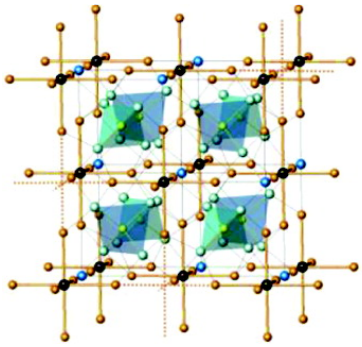

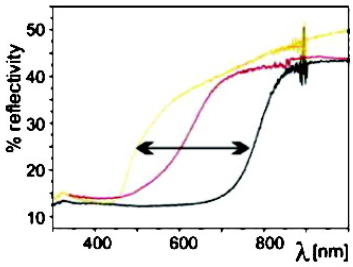

More About This Article

Additional resources and features associated with this article are available within the HTML version:

- Supporting Information
- Links to the 6 articles that cite this article, as of the time of this article download
- Access to high resolution figures
- Links to articles and content related to this article
- Copyright permission to reproduce figures and/or text from this article

View the Full Text HTML

J|A|C|S
ARTICLES
Published on Web 08/24/2005

Synthesis and Characterization of $[PtIn_6](GeO_4)_2O$ and Its Solid Solution $[PtIn_6](GaO_4)_{2-x}(GeO_4)_xO_{x/2}$ ($0 \le x \le 2$): Gradual Color Change of the Solid Solution from Black ($x = 0$) to Yellow ($x = 2$) as a Consequence of Quantum Dot Effect

Jürgen Köhler,*,† Holger Friedrich,† Myung-Hwan Whangbo,*,‡ and Antoine Villesuzanne‡,§

Contribution from the Max-Planck-Institut für Festkörperforschung, Stuttgart, Germany, and Department of Chemistry, North Carolina State University, Raleigh, North Carolina 27695-8204

Received May 19, 2005; E-mail: j.koehler@k.f.mpg.de; mike_whangbo@ncsu.edu

Abstract: A new phase $[PtIn_6](GeO_4)_2O$, a filled variant of $[PtIn_6](GaO_4)_2$, and the solid solution $[PtIn_6](GaO_4)_{2-x}(GeO_4)_xO_{x/2}$ ($0 \le x \le 2$) were prepared and characterized. Single-crystal structure refinements show that $[PtIn_6](GeO_4)_2O$ is isotypic with the mineral, sulfohalite $Na_6FCl(SO_4)_2$, and crystallizes in the space group $Fm\bar{3}m$ ($Z = 4$) with $a = 1006.0(1)$ pm. The building units of $[PtIn_6](GeO_4)_2O$ are isolated $[PtIn_6]^{10+}$ octahedra and $(GeO_4)^{4-}$ tetrahedra, and the isolated O^{2-} ions occupy the centers of the In_6 octahedra made up of six adjacent $PtIn_6$ octahedra. The lattice parameter of the solid solution $[PtIn_6](GaO_4)_{2-x}(GeO_4)_xO_{x/2}$ ($0 \le x \le 2$) varies gradually from $a = 1001.3(1)$ pm at $x = 0$ to $a = 1006.0(1)$ pm at $x = 2$, and the color of the solid solution changes gradually from black ($x = 0$) to red ($x = 1$) to yellow ($x = 2$). The cause for the gradual color change was examined by performing density functional theory electronic structure calculations for the end members $[PtIn_6](GaO_4)_2$ and $[PtIn_6](GeO_4)_2O$. Our analysis indicates that an oxygen atom at the center of a In_6 octahedron cuts the In 5p/In 5p bonding interactions between adjacent $[PtIn_6]^{10+}$ octahedra thereby raising the bottom of the conduction bands, and the resulting quantum dot effect is responsible for the color change.

1. Introduction

Low-valent indium oxides and fluorides are largely unknown, and all experiments to reduce InF_3 and In_2O_3 with H_2 or metallic In, which date back into the 1930s,[1] have failed. The low oxidation state of indium could be stabilized only in complex salts such as $InBF_4$ [2] containing isolated In^+ ions or $Na_{23}In_5O_{30}$ [3] and $In_5Mo_{18}O_{28}$ [4] with tetrahedral and linear In_5^{7+} Zintl cations, respectively. The structures of the recently discovered $PtIn_7F_{13}$,[5] $[PtIn_6](GaO_4)_2$, [6] and $Pt_2In_{14}Ga_3O_8F_{15}$ [7] contain highly positive $[PtIn_6]^{10+}$ octahedral clusters in which the low oxidation state of the indium atoms is stabilized by strong bonding interactions between In and Pt.[5,7] These clusters are counter examples of numerous electron-poor transition metal clusters encapsulating a main group element, which acts as an electron donor to stabilize metal−metal bonds and/or stabilizes the cluster by forming strong bonds between the metal and main group element.[8] Halides with octahedral clusters of main group or rare earth elements that are stuffed with a transition metal atom have also been found with the higher homologues iodine and bromine, e.g., $Cs_4Pr_6OsI_{13}$,[9] $K_4Pr_6I_{14}Os$,[10] $K_4La_6OsI_{14}$,[11] $Bi_{24}Ru_3Br_{20}$,[12] and $Bi_{34}Ir_3Br_{37}$.[13] With the lighter homologues chlorine and especially with fluorine, it is generally difficult to obtain such reduced phases because they are much less stable compared with phases containing metals in high oxidation states.[14] The same holds true for oxides, and only a few examples with Sn, e.g., $Ru_3Sn_{15}O_{14}$, [15] and $RuSn_6[(Al_{1/3-x}Si_{3x/4})O_4]_2$ ($0 \le x \le 1/3$),[16] are known so far.

$PtIn_7F_{13}$ and $Pt_2In_{14}Ga_3O_8F_{15}$ are colorless and transparent salt-like compounds that exhibit a high electrical resistivity. This

† Max-Planck-Institut für Festkörperforschung.
‡ Department of Chemistry, North Carolina State University.
§ Permanent address: ICMCB−CNRS, 87 Av. Dr. Schweitzer, 33608 Pessac cedex, France.

(1) Hannebohn, O.; Klemm, W. *Z. Anorg. Allg. Chem.* **1936**, *269*, 2.
(2) Fitz, H.; Müller, B. G. *Z. Anorg. Allg. Chem.* **1997**, *623*, 579.
(3) Deiseroth, H.-J.; Kerber, H.; Hoppe, R. *Z. Anorg. Allg. Chem.* **1998**, *624*, 541.
(4) Fais, E.; Borrmann, H.; Mattausch, H.-J.; Simon, A. *Z. Anorg. Allg. Chem.* **1995**, *621*, 1178.
(5) Köhler, J.; Chang, J.-H. *Angew. Chem.* **2000**, *112*, 2077; Köhler, J.; Chang, J.-H. *Angew. Chem., Int. Ed. Eng.* **2000**, *39*, 1998.
(6) Friedrich, H. A.; Köhler, J. *Z. Anorg. Allg. Chem.* **2001**, *627*, 144.
(7) Köhler, J.; Chang, J.-H.; Whangbo, M.-H. *J. Am. Chem. Soc.* **2005**, *127*, 2277.
(8) (a) Corbett, J. D. *Chem. Soc., Dalton. Trans.* **1996**, 575. (b) Simon, A. *Angew. Chem.* **1981**, *93*, 23; *Angew. Chem., Int. Ed. Engl.* **1981**, *20*, 1.
(9) Lulei, M.; Corbett, J. D. *Inorg. Chem.* **1996**, *35*, 4084.
(10) Uma, S.; Martin, J. D.; Corbett, J. D. *Inorg. Chem.* **1999**, *38*, 3825.
(11) Uma, S.; Corbett, J. D. *Inorg. Chem.* **1999**, *38*, 3831.
(12) Ruck, M. *Z. Anorg. Allg. Chem.* **1997**, *623*, 1591.
(13) Ruck, M. *Z. Anorg. Allg. Chem.* **1998**, *624*, 521.
(14) Johnson, D. A. *Some Thermodynamic Aspects of Inorganic Chemistry*, 2nd ed.; Cambridge University Press: Cambridge, 1982.
(15) Reichelt, W.; Söhnel, T.; Rademacher, O.; Oppermann, H.; Simon, A.; Mattausch, Hj.; Köhler, J. *Angew. Chem.* **1995**, *107*, 2307; Reichelt, W.; Söhnel, T.; Rademacher, O.; Oppermann, H.; Simon, A.; Mattausch, Hj.; Köhler, J. *Angew. Chem., Int. Ed. Engl.* **1995**, *34*, 2113.
(16) Söhnel, T.; Reichelt, W.; Wagner, F. E. *Z. Anorg. Allg. Chem.* **2000**, *626*, 223.

10.1021/ja053280x CCC: $30.25

is not surprising since the $[PtIn_6]^{10+}$ clusters are 18 electron species with a large energy gap between their HOMO (t_{1u}) and LUMO (e_g*) levels. Thus, it was surprising that the pentlandite-type variant $[PtIn_6](GaO_4)_2$, which is made up of $[PtIn_6]^{10+}$ octahedra and $(GaO_4)^{5-}$ tetrahedra, is black and semiconducting.[6] Our efforts to vary the charge of the $[PtIn_6]^{10+}$ octahedra in $PtIn_6(GaO_4)_2$ by substituting Ga by Ge has led to the discovery of the new germanate $PtIn_6(GeO_4)_2O$ and the solid solution $[PtIn_6](GaO_4)_{2-x}(GeO_4)_xO_{x/2}$ ($0 \le x \le 2$). To our surprise, the color of the solid solution changes gradually, i.e., from black at $x = 0$ to red at $x = 1.0$ to yellow at $x = 2$. In the present work, we describe our syntheses, crystal structure refinements and characterizations of $[PtIn_6](GeO_4)_2O$ and $[PtIn_6](GaO_4)_{2-x}(GeO_4)_xO_{x/2}$, and then explore why the solid solution changes its color gradually as a function of x on the basis of density functional theory (DFT) electronic band structure calculations for $[PtIn_6](GaO_4)_2$ and $[PtIn_6](GeO_4)_2O$.

2. Experimental Section

Synthesis. Carefully dried InF_3 (p.a. Merck) was first mixed with Pt powder (p.a. Merck), In powder (Alfa, 99.99%, 325 mesh), GeO_2 (Alfa, 99.99%) and Ga_2O_3 (Alfa, 99.99%) in stoichiometric amounts. The mixtures were ground in an agate mortar to a gray colored powder under Ar. Then the powder was pressed to a pellet, sealed under Ar in a Pt tube, and heated for 7 days at 1220 K. After cooling to room temperature (1 K/min), pale yellow transparent crystals of $[PtIn_6](GeO_4)_2O$ with a needlelike habit were found on the surface of the pellet. Pure powder samples of $[PtIn_6](GeO_4)_2O$ and $[PtIn_6](GaO_4)_{2-x}(GeO_4)_xO_{x/2}$ ($0 \le x \le 2$) were obtained by heating the pellets at 1200 K for 1 day, cooling to room temperature, grinding again, pressing a pellet and heating for another 2 days at 1200 K. The members of the series $[PtIn_6](GaO_4)_{2-x}(GeO_4)_xO_{x/2}$ ($0 \le x \le 2$) exhibit intense colors changing from black ($x = 0$) to red ($x = 1$) to yellow ($x = 1$) and are stable in air and insoluble in dilute HCl solution. The elemental analysis of a powder sample of $[PtIn_6](GeO_4)_2O$ with ICP[17] gave a Pt/In/Ge ratio of 1.0(1): 6.0(1): 2.0(1) in perfect agreement with the chemical formula. We did not perform chemical analyses for the members of the series $[PtIn_6](GaO_4)_{2-x}(GeO_4)_xO_{x/2}$ ($0 \le x \le 2$) because they were pure according to their powder X-ray diffraction patterns.

Structure Determination of $[PtIn_6](GeO_4)_2O$. The single-crystal X-ray investigation was performed on a Stoe IPDS diffractometer using Mo−Kα radiation (graphite monochromator). The intensities were corrected for Lorentz and polarization effects, and a semiempirical absorption correction was applied based on ψ-scans. The crystallographic characteristics and the experimental conditions of the data collection and refinement are summarized in Table S1 of the Supporting Information. All calculations were performed using SHELX programs.[18] Atomic scattering factors and anomalous dispersion corrections were taken from the 'International Tables for X-ray Crystallography'.[19] The structure of $[PtIn_6](GeO_4)_2O$ was refined in the space group $Fm\bar{3}m$ using the F^2 data with anisotropic displacement parameters for all atoms, to residuals wR2 = 0.042 for all 99 reflections, R1 = 0.016 for 1210 reflections with $I > 2\sigma(I)$ (see Tables S1 and S2 of the Supporting Information). Table 1 presents the final results for the refined atomic positions and isotropic displacement factors for $[PtIn_6](GeO_4)_2O$.[20] Some interatomic distances are given in Table 2.

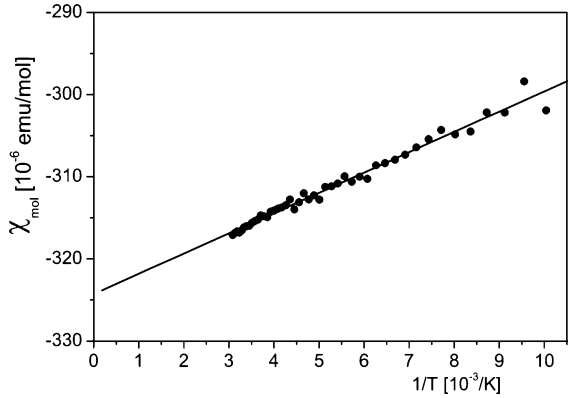

Figure 1. Molar susceptibility χ_{mol} of $[PtIn_6](GeO_4)_2O$ as a function of the reciprocal temperature in the range of 100−330 K.

Table 1. Positional Parameters and Isotropic Displacement Factors (pm^2) for $[PtIn_6](GeO_4)_2O$[a]

atom	Wyckoff position	x	y	z	U_{iso}
Pt	4*a*	0	0	0	0.0045(2)
In	24*e*	0.2606(1)	0	0	0.0062(2)
Ge	8*c*	1/4	1/4	1/4	0.0043(3)
O(1)	32*f*	0.3506(3)	x	x	0.0077(9)
O(2)	4*b*	1/2	0	0	0.0080(9)

[a] The space group is $Fm\bar{3}m$ (No. 225), and the cell parameter a = 1006.0(1) pm.

Table 2. Interatomic Distances (pm) of $[PtIn_6](GeO_4)_2O$

Pt	- In	262.1(1) (6×)	O1	- Ge	175.2(5) (1×)
				- In	231.1(3) (3×)
In	- O1	231.1(3) (4×)		- O1	286.1(6) (3×)
	- O2	240.9(1) (1×)		- O1	300.7(8) (3×)
	- Pt	262.1(1) (1×)		- O2	260.4(3) (1×)
	- In	340.7(1) (4×)			
	- In	370.7(1) (4×)			
			O2	- In	240.9(1) (6×)
Ge	- O1	175.2(5) (4×)	O2	- O1	260.4(3) (8×)

Magnetic Susceptibility Measurement. The magnetic susceptibility of $[PtIn_6](GeO_4)_2O$ was measured as a function of temperature using a SQUID susceptometer at a constant external magnetic field of 5 T. Figure 1 shows the molar susceptibility χ_{mol} as a function of the reciprocal temperature in the range of 100−330 K. The measurements reveal that $[PtIn_6](GeO_4)_2O$ is diamagnetic, and the extrapolation of the magnetic susceptibility for $1/T \rightarrow 0$ results in a value of $-324(15) \times 10^{-6}$ emu/mol, in agreement with the expected value of -264×10^{-6} emu/mol from the diamagnetic contributions of the constituent atoms (O^{2-}: -12×10^{-6} emu/mol; Ge^{4+}: -7×10^{-6} emu/mol; In^{3+}: -19×10^{-6} emu/mol; Pt^{4+}: -28×10^{-6} emu/mol).[21]

Electronic Structure Calculations. First principles DFT calculations were carried out with the full-potential augmented-plane-wave + local orbitals (APW+lo) method[22,23] implemented in the WIEN2k code[24] using the generalized gradient approximation (GGA) of Perdew, Burke and Ernzerhof.[25] The valence states were described by scalar relativistic wave functions without spin−orbit coupling. The muffin-tin radii used were 2.3 au for Pt and In atoms, and 1.65 au for Ge, Ga, and O atoms. The plane-wave cutoff was $R_{MT} \cdot K_{max} = 7$, and 16 k-points were used

(17) Buresch, O.; Schnering, H. G. v. *Fresenius Z. Anal. Chem.* **1984**, *319*, 418.
(18) Sheldrick, G. M. *SHELX-97*, Program for the refinement of crystal structures from diffraction data, University of Göttingen: Germany, 1997.
(19) Hahn, T., Ed. *International Tables of Crystallography*, 4th ed.; Kluwer: Dordrecht, 1995; Vol. A.
(20) Further details of the crystal structure investigation may be obtained from the Fachinformationzentrum Energie, Physik, Mathematik, D-76344 Eggenstein-Leopoldshafen 2, on quoting the depository number CSD-415405, the names of the authors, and the journal citation.
(21) Selwood, P. W. *Magnetochemistry*, 2nd ed.; Interscience: New York, 1956.
(22) Sjöstedt, E.; Nordström, L.; Singh, D. *Solid State Commun.* **2000**, *114*, 15.
(23) Madsen, G. K. H.; Blaha, P.; Schwarz, K.; Sjöstedt, E.; Nordström, L. *Phys. Rev. B* **2001**, *64*, 195134.
(24) Blaha, P.; Schwarz, K.; Madsen, G. K. H.; Kvasnicka, D.; Luitz, J. WIEN2k, *An Augmented Plane Wave Plus Local Orbitals Program for Calculating Crystal Properties*; Vienna University of Technology, Austria, 2001; ISBN 3-9501031-1-2.
(25) Perdew, J. P.; Burke, K.; Ernzerhof, M. *Phys. Rev. Lett.* **1996**, *77*, 3865.

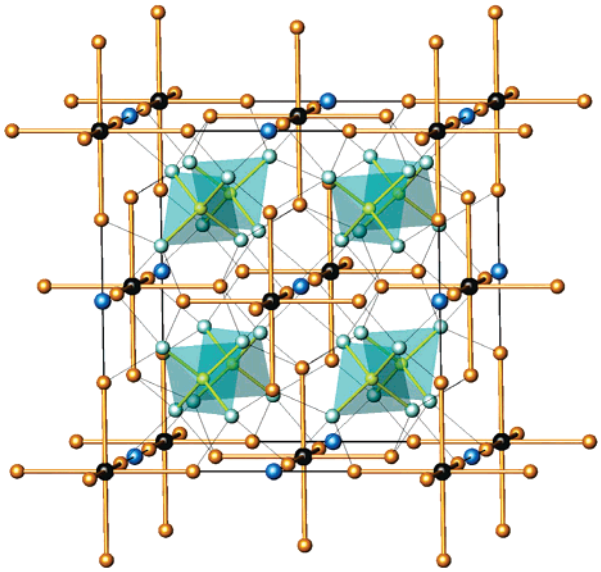

Figure 2. Perspective view of the crystal structure of $[PtIn_6](GeO_4)_2O$ emphasizing the building blocks. The $[PtIn_6]^{10+}$ octahedra and $[GeO_4]^{4-}$ tetrahedra are graphically emphasized. The black spheres correspond to the Pt atoms, the orange spheres to the In atoms, the yellowish-green spheres to the Ge atoms, and the light and dark blue spheres to the O(1) and O(2) atoms, respectively.

for the sampling of the irreducible wedges of the Brillouin zones. The electronic structures of the $PtIn_6$ cluster of $[PtIn_6](GeO_4)_2O$, were calculated by extended Hückel tight binding (EHTB) calculations.[26] The structures of the $PtIn_6$ were taken to be regular octahedra using the average Pt−In bond lengths. The Pt 5d and In 5s/5p orbitals were represented by double-ζ Slater type orbitals.[27] The atomic parameters used for calculations were the same as those employed in ref 7.

3. Crystal Structure

$[PtIn_6](GeO_4)_2O$. The cubic structure of $[PtIn_6](GeO_4)_2O$ contains $PtIn_6$ octahedra and GeO_4 tetrahedra, which are arranged like the Ca and F atoms in CaF_2. The additional O atoms occupy the 4*b* position on the edges and in the center of the F centered unit cell (Figure 2). The GeO_4 tetrahedra are regular with four Ge−O(1) bond distances of 175.2 pm (Table 2), which are comparable to those of *ortho*-oxogermanates, e.g., K_4GeO_4.[28] The calculated bond valence sum ($B = 37$, $r_0 = 174.8$ pm)[29] for the Ge atoms in $[PtIn_6](GeO_4)_2O$ is 3.96. Thus, with the reasonable oxidation states +4 for Ge and −2 for O, the charge balance requirement for $[PtIn_6](GeO_4)_2O$ leads to a charge of +10 for the $PtIn_6$ octahedra, as in other compounds $PtIn_7F_{13}$,[5] $PtIn_6Ga_2O_8$ [6] and $Pt_2In_{14}Ga_3O_8F_{15}$ [7] containing $PtIn_6$ octahedra. (It is noted that the charge balance of the mineral sulfohalite $Na_6FCl(SO_4)_2$, to which the crystal structure of $[PtIn_6](GeO_4)_2O$ belongs, can be written as $[FNa_6]^{5+}([SO_4]^{2-})_2(Cl^-)$).[30] As shown in Figure 3, the structure of $[PtIn_6](GeO_4)_2O$ can also be described in terms of a cubic close packing of the metal atoms In and Ge in which one-fourth of the octahedral holes are occupied by Pt and O(2), and half the tetrahedral holes by O(1). This description points out that the role of the Pt atoms

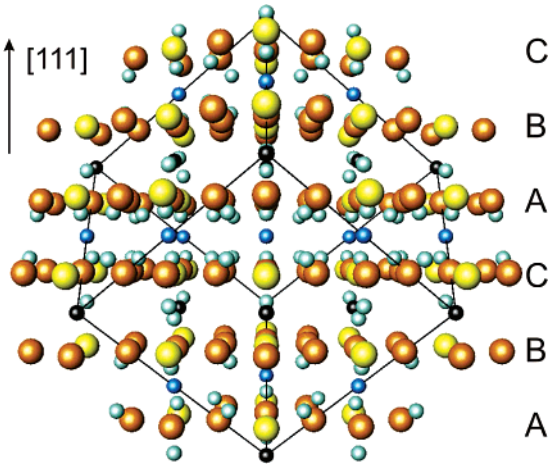

Figure 3. Perspective view of the structure of $[PtIn_6](GeO_4)_2O$ from the viewpoint of a cubic close packing of atoms.

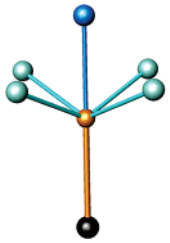

Figure 4. Perspective view of an $In[PtO(1)_4O(2)]$ polyhedron in $[PtIn_6](GeO_4)_2O$.

in this structure is comparable to the O atoms, hence indicating an anionic character of Pt (see below).

The Pt−In distances within the $PtIn_6$ octahedra of $[PtIn_6](GeO_4)_2O$ are 262 pm and are relatively short compared with intermetallic phases with six-coordinate Pt, e.g., $LaPtIn_3$ [31] (Pt−In = 269 pm) and $Sr_2Pt_3In_4$ [32] (Pt−In = 265 pm). However, they are longer than those found for the $PtIn_6$ clusters in $PtIn_7F_{13}$ [5] (253.0 and 254.7 pm), $[PtIn_6](GaO_4)_2$ [6] (253.5 pm) and $Pt_2In_{14}Ga_3O_8F_{15}$ (253.5 pm).[7] The In−In distances within each $PtIn_6$ octahedron of $[PtIn_6](GeO_4)_2O$ are 370 pm, and are longer than those in elemental In (325 pm − 338 pm). As depicted in Figure 4, each In is surrounded by one Pt, four O(1) atoms and one O(2), and the In atom is displaced by ∼11 pm out of the plane of the four O(1). The bond valence sum calculated for In (with B = 37 and $r_0 = 190.2$ pm derived for $In^{3+}-O^{2-}$ distances) is 1.58, which indicates an oxidation state lower than +3.

As depicted in Figure 5, each $PtIn_6$ octahedron is surrounded by as many as 30 O^{2-} anions to form a $[PtIn_6]O_{30}$ unit. Such a high number of ligands around each $PtIn_6$ cluster in $[PtIn_6](GeO_4)_2O$, which is the largest found for an octahedral unit, can be understood because the ratio of the average In−In distance to the average In−O distance is large (∼1.7). As a comparison, we note that each Nb_6 cluster of reduced oxoniobates has 18 O ligands, and the ratio of the Nb−Nb to the Nb−O average distance is ∼1.4.[33]

Each O(1) atom is tetrahedrally coordinated by one Ge and three In atoms. The O(2) atoms are located at the center of In_6

(26) Our calculations were carried out by employing the SAMOA (Structure and Molecular Orbital Analyzer) program package (Dai, D.; Ren, J.; Liang, W.; Whangbo, M.-H., http://chvamw.chem.ncsu.edu/, 2002).
(27) Clementi, E.; Roetti, C. *Atomic Data Nuclear Data Tables* **1974**, *14*, 177.
(28) Hoch, C.; Roehr, C. *Z. Naturforsch B.* **2001**, *56*, 1245; Nowitzki, B.; Hoppe, R. *Z. Anorg. Allg. Chem.* **1983**, *505*, 105.
(29) Brown, I. D.; Altermatt, D. *Acta Crystallogr.* **1985**, *B41*, 244.
(30) Sakamoto, Y. *J. Science Hiroshima University* **1968**, *A32*, 101.
(31) Galadzhun, Y. V.; Pöttgen, R. *Z. Anorg. Allg. Chem.* **1998**, *625*, 481.
(32) Hoffmann, R.-D.; Pöttgen, R. *Z. Anorg. Allg. Chem.* **1998**, *625*, 994.
(33) Köhler, J.; Svensson, G.; Simon, A. *Angew. Chemie.* **1992**, *104*, 1463. Köhler, J.; Svensson, G.; Simon, A. *Angew. Chem., Int. Ed. Eng.* **1992**, *31*, 1437.

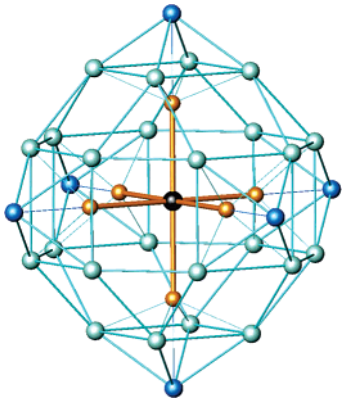

Figure 5. Perspective view of a $[PtIn_6]O_{30}$ polyhedron in $[PtIn_6](GeO_4)_2O$.

octahedra made up of six different $PtIn_6$ octahedra, with O(2)−In distance of 241 pm. An octahedral coordination of an O(2) atom by indium is rather unusual, and the In−O(2) distances are in the same range in a few known complex of In^{3+}, i.e., In−O = 236 pm (4×) and 249 pm (2×) in $BaNi_2In_8O_{15}$,[34] and In−O = 235 pm (4×) and 245 pm (2×) in $BaNi_2In_4Sc_4O_{15}$.[35]

Solid Solution $[PtIn_6](GaO_4)_{2-x}(GeO_4)_xO_{x/2}$ ($0 \le x \le 2$). The structure of $[PtIn_6](GeO_4)_2O$ is closely related to the pentlandite type structure of $[PtIn_6](GaO_4)_2$.[6] Both oxides crystallize in the space group $Fm\bar{3}m$ with lattice constants a = 1006.0(1) and 1001.3(1) pm, respectively. The main difference is that in $PtIn_6Ge_2O_9$ the center of every In_6 octahedron made up of six adjacent $[PtIn_6]$ octahedra is occupied by an O(2) atom, whereas in $[PtIn_6](GaO_4)_2$ this site is empty (Figure 2). Therefore, $[PtIn_6](GeO_4)_2O$ is a filled variant of the pentlandite. As mentioned above, the Pt−In distances of $[PtIn_6](GeO_4)_2O$ are longer than those of $[PtIn_6](GaO_4)_2$ by 9 pm, whereas the GeO_4 tetrahedra are smaller than the GaO_4 tetrahedra (Ge−O = 175 pm, Ga−O = 187 pm). The In−O distances between the $PtIn_6$ octahedra and the MO_4 (M = Ge, Ga) tetrahedra are 231 pm for M = Ge, and 226 pm for M = Ga. The $[O(2)In_6]$ octahedra of $[PtIn_6](GeO_4)_2O$ exhibit 12 In−In distances of 340 pm, and are contracted compared with the empty In_6 octahedra of $PtIn_6Ga_2O_8$ in which In−In = 350 pm, i.e., the In−In distance between $PtIn_6$ clusters is longer in $[PtIn_6](GaO_4)_2$ than in $[PtIn_6](GeO_4)_2O$.

The cubic lattice constant of the solid solution $[PtIn_6](GaO_4)_{2-x}(GeO_4)_xO_{x/2}$ ($0 \le x \le 2$) changes gradually from a = 1001.3(1) pm ($x = 0$) to a = 1006.0(1) pm ($x = 2$) as shown in Figure 6. The cell parameter does not vary linearly with x, because there are two competing size effects, i.e., the contraction of the tetrahedral cluster in average and the expansion of the $PtIn_6$ octahedral cluster in average (see above). What is most striking is the color change that occurs as a function of x, as shown in Figure 7. The corresponding reflectivity spectra show that approximately 85% of the incident light is absorbed below 800 nm for $x = 0$ (i.e., $[PtIn_6](GaO_4)_2$), and that the absorption edge is shifted toward shorter wavelengths with increasing x (Figure 8).

4. Electronic Structure and Color Change

$[PtIn_6]^{10+}$ Cation. A detailed discussion of the bonding of the highly positive $[PtIn_6]^{10+}$ clusters was given in the studies of $Pt_2In_{14}Ga_3O_8F_{15}$ [7] and $PtIn_7F_{13}$.[5] Our EHTB calculations show that an isolated $[PtIn_6]^{10+}$ octahedron of $[PtIn_6](GeO_4)_2O$ has very similar molecular orbitals (MO's) as does that of $Pt_2In_{14}Ga_3O_8F_{15}$.[7] The low-lying MO's of $[PtIn_6]^{10+}$ are largely made up of the Pt 5d/6s/6p and the In 5s orbitals. The calculated MO levels increase in the order $1e_g$, $1t_{2g}$, $1a_{1g} < 1t_{1u} < 2e_g < 2a_{1g}$. With 18 valence electrons per $[PtIn_6]^{10+}$ ion, the $1e_g$, $1t_{2g}$, $1a_{1g}$,

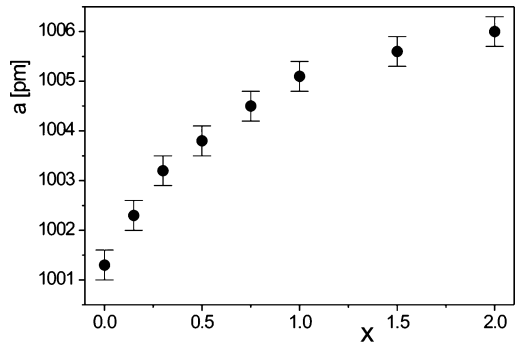

Figure 6. Lattice constant a of the solid solution $[PtIn_6](GaO_4)_{2-x}(GeO_4)_xO_{x/2}$ ($0 \le x \le 2$) as a function of x.

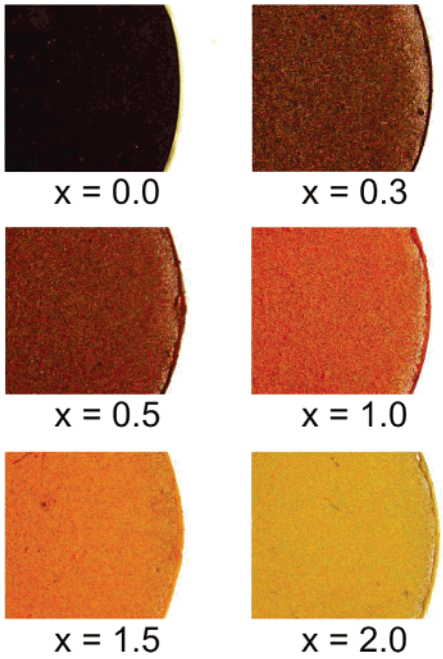

Figure 7. Colors of the solid solution $[PtIn_6](GaO_4)_{2-x}(GeO_4)_xO_{x/2}$ ($0 \le x \le 2$).

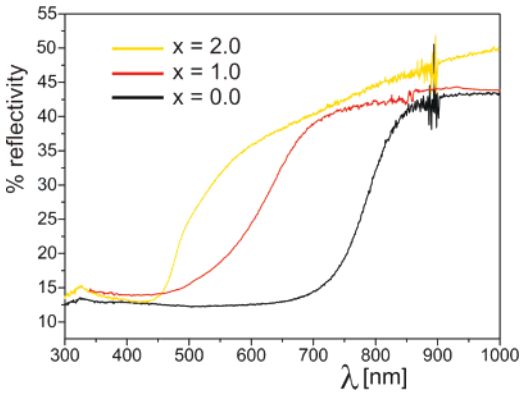

Figure 8. Reflectivity spectra of compounds of the solid solution $[PtIn_6](GaO_4)_{2-x}(GeO_4)_xO_{x/2}$ ($0 \le x \le 2$).

(34) Schiffler, S.; Müller-Buschbaum, Hk. *Z. Anorg. Allg. Chem.* **1986**, *542*, 25.
(35) Müller-Buschbaum, Hk.; Rüter, I. *Z. Anorg. Allg. Chem.* **1989**, *572*, 109.

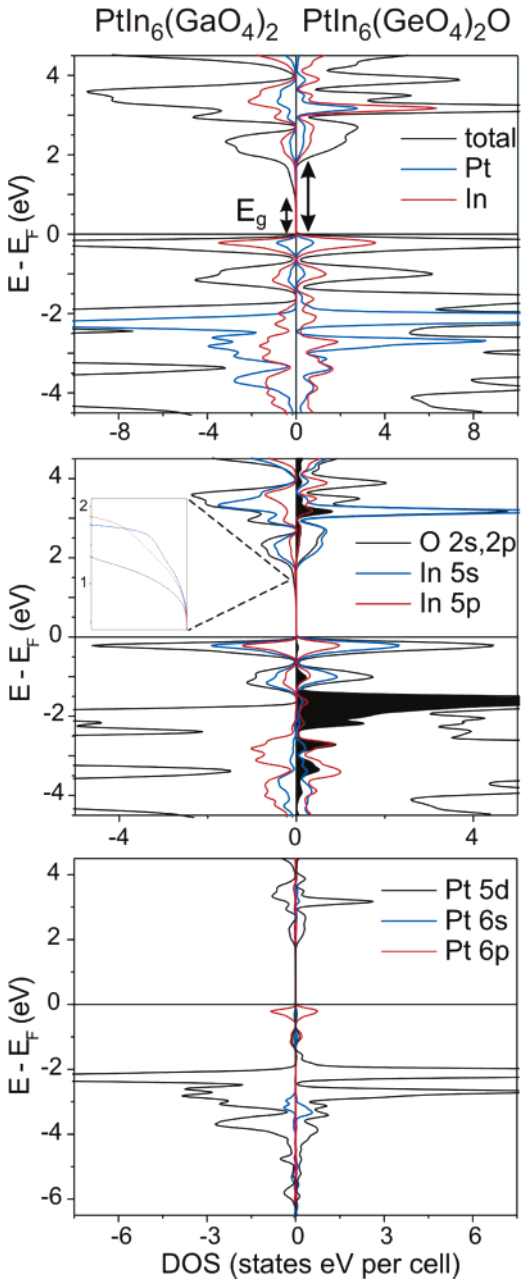

Figure 9. Total and partial DOS plots calculated with the APW+lo method for $[PtIn_6](GaO_4)_2$ and $[PtIn_6](GeO_4)_2O$. The inset for $[PtIn_6](GeO_4)_2O$ shows a zoomed-in view of the bottom of the conduction band. The partial DOS plot for the O(2) atom is shaded.

and $1t_{1u}$ levels (nine altogether) are completely filled while the $2e_g$ and $2a_{1g}$ levels are empty, hence leading to the oxidation state −2 for Pt.[7] The latter might appear unusual, but Pt is more electronegative than In,[36] and the In 5s level lies higher in energy than the Pt 5d level.[27,37] Furthermore, the recently discovered compound Cs_2Pt [38] with red color supports the possibility that the oxidation state of Pt can be −2. In $[PtIn_6]^{10+}$, the Pt 5d orbitals act as a reservoir for holding 10 electrons, and the essential bonding between Pt with its surrounding In ligands takes place by use of the 6s and 6p orbitals of Pt.[7] A similar

(36) http://www.webelements.com/.
(37) Paradis, J. A.; Whangbo, M.-H.; Kasowski, R. V. *New J. Chem.* **1993**, *17*, 525.
(38) Karpov, A. S.; Nuss, J.; Wedig, U.; Jansen, M. *Angew. Chem.* **2003**, *115*, 4966; *Angew. Chem., Int. Ed. Engl.* **2003**, *42*, 4818.

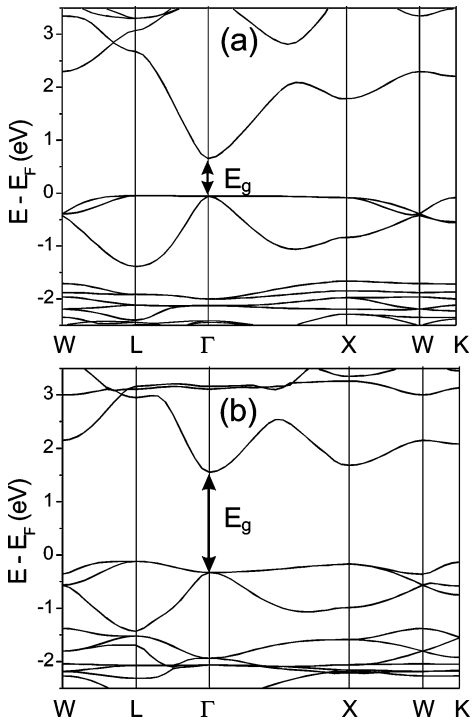

Figure 10. Dispersion relations of the bands around the band gap calculated with the APW+lo method for (a) $[PtIn_6](GaO_4)_2$ and (b) $[PtIn_6](GeO_4)_2O$. The Brillouin zone and high symmetry points are shown in Figure S1 of the Supporting Information.

picture of bonding was found from the electronic structure studies on the highly negative anions $[MIn_{10}]^{10-}$ of $K_{10}In_{10}M$ (M = Ni, Pd, Pt).[39]

Electronic Band Structures of $[PtIn_6](GeO_4)_2O$ and $PtIn_6(GaO_4)_2$. The plots of the total and partial density of states (DOS) calculated for $[PtIn_6](GeO_4)_2O$ and $[PtIn_6](GaO_4)_2$ are compared in Figure 9. The bands of the Pt 5d orbital character lie well below the Fermi level, i.e., all the Pt 5d levels are completely filled. In addition, the population of the Pt 6s/6p orbitals calculated from integrating the partial DOS plots is approximately 0.7 electrons. The latter amounts to approximately 1.4 electrons around Pt, given the covalent bonding between Pt and In.[7] Thus, the oxidation state for the Pt in the $[PtIn_6]^{10+}$ cation is close to −2, as already discussed.[7]

The dispersion relations of the bands around the band gaps are presented in Figure 10. The bottom of the conduction bands occurs at the Γ point, and the band gaps of $[PtIn_6](GaO_4)_2$ and $[PtIn_6](GeO_4)_2O$ are calculated to be 0.7 and 1.7 eV, respectively. These gaps should be compared with the experimental values 1.2 − 1.5 eV for $[PtIn_6](GaO_4)_2$, and 2.2 − 2.5 eV for $[PtIn_6](GeO_4)_2O$. Thus, the present DFT calculations underestimate the band gaps, which is a well-known deficiency of DFT calculations. Nevertheless, the calculated band gap is greater for $[PtIn_6](GeO_4)_2O$ than for $[PtIn_6](GaO_4)_2$ by approximately 1 eV, in good agreement with the corresponding difference in the experimental band gaps. The band gap is indirect in $[PtIn_6](GeO_4)_2O$.

The bottom of the conduction bands of $[PtIn_6](GaO_4)_2$ are represented by the In 5s and 5p orbitals (see the inset of Figure 9). The lowest unoccupied crystal orbital (LUCO) of $[PtIn_6](GaO_4)_2$ occurs at the Γ point, where the In $5p_x$, $5p_y$, and $5p_z$

(39) Sevov, S. C.; Corbett, J. D. *J. Am. Chem. Soc.* **1993**, *115*, 9089.

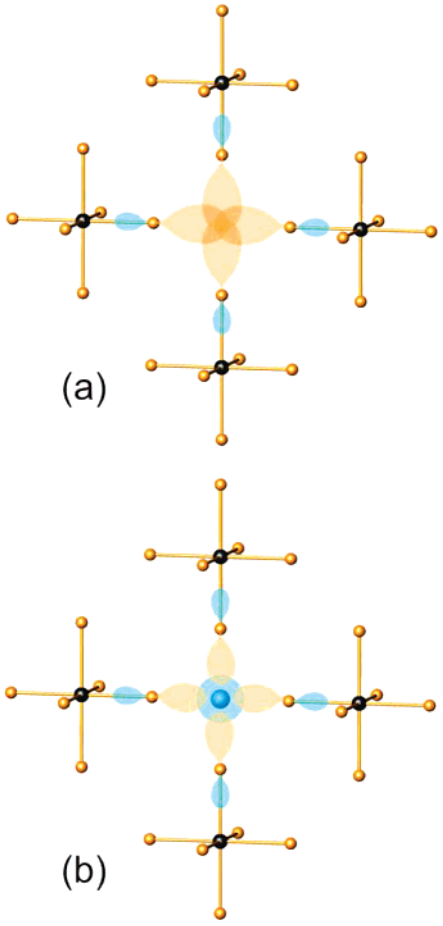

Figure 11. Schematic representation of the overlap between the In 5p orbitals of (a) an empty In_6 octahedron and (b) a filled In_6 octahedron with O(2). For simplicity, the two $PtIn_6$ octahedra above and blow the O(2) atom were omitted.

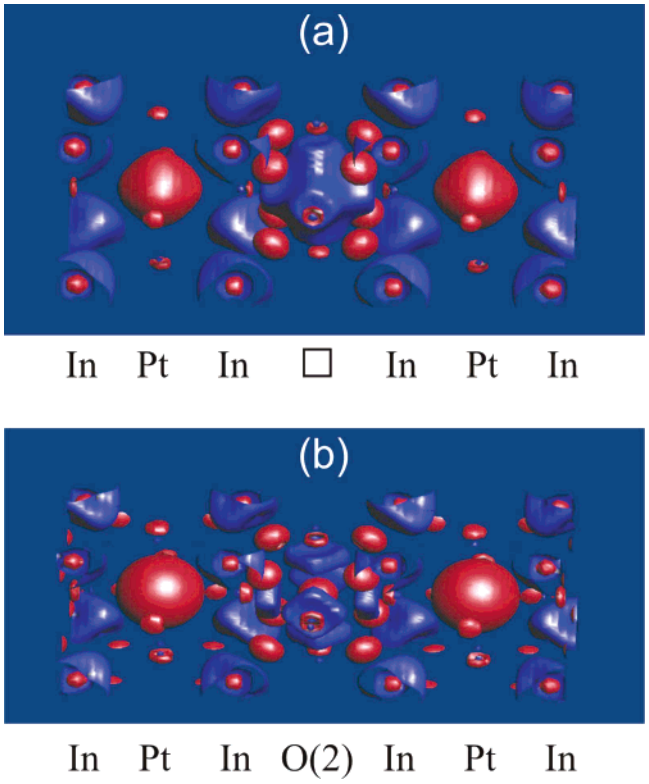

Figure 12. Boundary surface density plots calculated with the APW+lo method for (a) the LUCO level of $PtIn_6Ga_2O_8$ in the region of an empty O(2) site and (b) the LUCO level of $[PtIn_6](GeO_4)_2O$ in the region of an O(2) site.

orbitals of each empty In_6 octahedron make sigma bonding interactions along the a-, b-, and c-directions, respectively, (i.e., across the three diagonal directions of the empty In_6 octahedron) such that their maximum overlap occurs at the empty extra oxygen sites (Figure 11a). In other words, these interactions represent sigma bonding interactions between adjacent $PtIn_6$ octahedra along the a-, b-, and c-directions. This is shown by the boundary surface plot for the LUCO of $[PtIn_6](GaO_4)_2$ presented in Figure 12a, where the red and blue colors represent different signs of the boundary surfaces. The red spheres are located at the Pt atom sites, and the blue "octahedra" at the extra oxygen sites. In lowering the bottom of the conduction bands of $[PtIn_6](GaO_4)_2$ at the Γ point, the sigma bonding interaction between adjacent $PtIn_6$ cluster is necessary. Therefore, the shortest In···In distance between adjacent $PtIn_6$ cluster should be short enough that the sigma overlap between the In 5p orbitals becomes significant. This distance is 350 pm and the trans In···In distance is $\sqrt{2} \times 350 = 495$ pm in $[PtIn_6](GaO_4)_2$, which is rather short considering the large spatial extension of the In 5s and 5p orbitals. In $PtIn_7F_{13}$ and $Pt_2In_{14}Ga_3O_8F_{15}$, such In···In interactions do not occur due to the way their $PtIn_6$ octahedra are arranged.

In $[PtIn_6](GeO_4)_2O$, the extra oxygen sites are all occupied by oxygen. At the Γ point, the bottom of the conduction bands of $[PtIn_6](GeO_4)_2O$ is also represented by the sigma bonding interactions of the In 5p orbitals between adjacent $PtIn_6$ clusters along the a-, b-, and c-directions. However, the In 5p orbitals are forced by symmetry to make antibonding interactions with the O 2s orbitals of the extra oxygen sites (Figure 11b), thereby raising the bottom of the conduction bands hence increasing the band gap by ~1 eV. This is shown by the boundary surface plot for the LUCO of $[PtIn_6](GeO_4)_2O$ presented in Figure 12b. The trans In···In distances within each $O(2)In_6$ octahedron of $[PtIn_6](GeO_4)_2O$ are 480 pm, i.e., shorter than those within the empty In_6 octahedron of $[PtIn_6](GaO_4)_2$ (495 pm). This is explained by the strong electrostatic and covalent O(2)−In bonding interactions in the valence bands.

Color Change in $[PtIn_6](GaO_4)_{2-x}(GeO_4)_xO_{x/2}$. $[PtIn_6](GeO_4)_2O$ consists of diamagnetic ions $[PtIn_6]^{10+}$, $[GeO_4]^{4-}$, and O^{2-}, in agreement with its diamagnetism and its yellow color. As a function of x, the solid solution $[PtIn_6](GaO_4)_{2-x}(GeO_4)_xO_{x/2}$ ($0 \le x \le 2$) changes its color gradually from black ($x = 0$) to red ($x = 1$) to yellow ($x = 2$). According to our DFT electronic band structure calculations for the end members $[PtIn_6](GaO_4)_2$ and $[PtIn_6](GeO_4)_2O$, the color change in the solid solution $[PtIn_6](GaO_4)_{2-x}(GeO_4)_xO_{x/2}$ ($0 \le x \le 2$) can be explained as follows: (a) The substitution of two GeO_4 tetrahedra for two GaO_4 tetrahedra is accompanied by one O in the extra oxygen sites. (b) An O atom in an extra oxygen site has the role of cutting the sigma bonding interaction between the In 5p orbitals of adjacent $PtIn_6$ octahedra along the a-, b-, and c-directions. (c) Therefore, as far as the conduction bands (made up of the In 5s/5p orbitals) are concerned, the effective crystal size becomes smaller when the extra oxygen sites are occupied with O. (d) With increasing x, therefore, smaller "quantum dots" are

produced.[40] Therefore, the band gap increases with increasing x.

The observed color change in $[PtIn_6](GaO_4)_{2-x}(GeO_4)_xO_{x/2}$ ($0 \le x \le 2$) as a function of x is well explained by the above. The above explanation also predicts that the solid solution $[PtIn_6](GaO_4)_{2-x}(GeO_4)_xO_{x/2}$ ($0 \le x \le 2$) should be diamagnetic, not paramagnetic. An oxygen impurity idea cannot explain the gradual color change that occurs as a function of x, because it predicts that these compounds are paramagnetic.

5. Concluding Remarks

The new phase $[PtIn_6](GeO_4)_2O$ is a filled variant of $[PtIn_6](GaO_4)_2$. $[PtIn_6](GaO_4)_2$ has empty In_6 octahedra made up of six adjacent $PtIn_6$ octahedra, and the centers of such In_6 octahedra are occupied by the additional O atoms in $[PtIn_6](GeO_4)_2O$. The color of the solid solution $[PtIn_6](GaO_4)_{2-x}(GeO_4)_xO_{x/2}$ ($0 \le x \le 2$) changes gradually from black ($x = 0$) to red ($x = 1$) to yellow ($x = 2$). Our electronic band structure calculations for $[PtIn_6](GaO_4)_2$ and $[PtIn_6](GeO_4)_2O$ show that an oxygen atom at each In_6 octahedral void cuts the In 5p/In 5p sigma bonding interactions between the $[PtIn_6]^{10+}$ octahedra surrounding the oxygen. This raises the bottom of the conduction bands, and the resulting quantum dot effect causes the gradual color change of the solid solution.

Acknowledgment. The authors thank E. Brücher for the measurement of the magnetic susceptibility. M.-H. W. thanks the financial support from the Office of Basic Energy Sciences, Division of Materials Sciences, U. S. Department of Energy, under Grant No. DE-FG02-86ER45259. A. V. thanks the Pole M3PEC, Bordeaux 1 University, France, for computational resources.

Supporting Information Available: The crystallographic data and parameters of data collection and structure refinements of $[PtIn_6](GeO_4)_2O$ (Table S1), the anisotropic displacement factors for $[PtIn_6](GeO_4)_2O$ (Table S2), and the Brillouin zone and its high symmetry points for a face-centered cubic lattice (Figure S1). This material is available free of charge via the Internet at http://pubs.acs.org.

JA053280X

(40) For reviews, see: (a) Bawendi, M. G.; Steigerwald, M. L.; Brus, L. E. *Annu. Rev. Phys. Chem.* **1990**, *41*, 477. (b) Norris, D. J.; Bawendi, M. G.; Brus, L. E. *Molecular Electronics* **1997**, 281. (c) Ashoori, R. C. *Nature* **1996**, *379*, 413.